Magnetic and Magnetostrictive Behavior of Iron-Silicon Single Crystals Under Uniaxial Stress

Karl-Joseph Rizzo[1,2], Olivier Hubert[1], and Laurent Daniel[2]

[1]LMT-Cachan ENS-Cachan/CNRS/UPMC/UniverSud Paris, Cachan cedex F-94235, France
[2]LGEP Supelec/CNRS/Univ Paris-Sud/UPMC, Gif-sur-Yvette Cedex F-91192, France

This paper presents the full characterization of the reversible magneto-mechanical behavior of iron-silicon single crystals. Magnetostriction and magnetization measurements under tensile mechanical loading have been performed on specimen collected along the $\langle 100\rangle$, $\langle 110\rangle$ and $\langle 111\rangle$ crystallographic axes. A theoretical interpretation of the results is attempted.

***Index Terms*—Magnetoelasticity, silicon steel.**

I. Introduction

THE search for weight optimization of electromechanical systems leads to build more compact and high speed systems. These systems generate high levels of multiaxial mechanical stress, that strongly change the magnetic behavior of materials. In order to reach optimal design for electromagnetic devices, this magneto-mechanical coupling effect need to be introduced in advanced modeling tools. Macroscopic phenomenological approach (see for instance [1]) does not provide a sufficient description of such complex phenomena. An alternative way is the requirement of multiscale approaches introducing the coupling effect at the single crystal scale [2], and considering the effect of stress on the magnetic domains distribution. The full characterization of the magneto-mechanical behavior of single crystals is the first step necessary for the development of such a multiscale approach. We present in this paper the measurements of reversible magnetic and magnetostrictive behavior of an iron-silicon steel (3%Si-Fe) single crystal cut along the $\langle 100\rangle$, $\langle 110\rangle$ and $\langle 111\rangle$ crystallographic axes. Samples are submitted to both a magnetic excitation and a mechanical tensile loading. In a second part, these results are discussed from a theoretical point of view.

II. Magneto-Mechanical Characterization

An industrial grain-oriented silicon steel (3%Si-Fe GO, 0.3 mm thick) has been used for the experiments. This material exhibits a very large grain size (around 40 mm) and a strong crystallographic GOSS texture (rolling direction (RD)//[001], transverse direction (TD)//[$\bar{1}$10]) [3]. 200 mm long and 12.5 mm wide bands have been cut in sheet at 0°, 90° and 54.7° from RD, ideally corresponding to the crystallographic axes $\langle 100\rangle$, $\langle 110\rangle$ and $\langle 111\rangle$. The cutting area has been selected so that a large grain stands in the middle of the sample (see Fig. 1). The strips are equipped with heads in order to apply a pure mechanical tensile loading using weights. The selected grain is equipped with a pick-up coil for magnetic induction measurement. Strain gages are stuck on both sides of the sample in order to measure the magnetostriction along sample length and width. A specific procedure allows the measurement of the anhysteretic behavior of the material [4].

Fig. 1. Specimen, view of grain, coil and strain gage.

The anhysteretic magnetization and magnetostriction measurements in stress free conditions are presented in Fig. 2. The results obtained under tensile stress are presented in Fig. 3 for the three directions 0°, 90° and 54.7°. We note $\Delta\lambda_{//}$ the deformation measured along the sample length and $\Delta\lambda_{\perp}$ the deformation measured along the sample width.

III. Results Interpretation

The interpretation of these measurements is based on a schematic representation of the domain configuration and its evolution under external magneto-mechanical loading (Fig. 4). This schematic interpretation has already been presented in stress free configurations [3] (Fig. 4(b)–(i)) and is extended here to the case where a tensile stress is applied in free magnetic field configurations (Fig. 4(b')–(i')).

We focus on the relationship between the change of the magnetic domain structure and the measured magnetostriction. A domain α is an area inside the single crystal with uniform magnetization $\vec{M}_\alpha$ and uniform magnetostriction strain ε_μ^α given by (1) and (2)

$$\vec{M}_\alpha = M_S\vec{\gamma}_\alpha = M_S{}^t[\gamma_1\ \gamma_2\ \gamma_3] \tag{1}$$

$$\varepsilon_\mu^\alpha = \frac{3}{2}\begin{pmatrix} \lambda_{100}\left(\gamma_1^2-\frac{1}{3}\right) & \lambda_{111}\gamma_1\gamma_2 & \lambda_{111}\gamma_1\gamma_3 \\ \lambda_{111}\gamma_1\gamma_2 & \lambda_{100}\left(\gamma_2^2-\frac{1}{3}\right) & \lambda_{111}\gamma_2\gamma_3 \\ \lambda_{111}\gamma_1\gamma_3 & \lambda_{111}\gamma_2\gamma_3 & \lambda_{100}\left(\gamma_3^2-1\frac{1}{3}\right) \end{pmatrix}_{\mathrm{CF}}. \tag{2}$$

M_S is the saturation magnetization of the material, $\vec{\gamma}_\alpha$ the direction of the magnetization in the domain α, with direction cosines γ_1, γ_2, and γ_3 in the crystallographic frame CF. λ_{100} and λ_{111} are the magnetostriction constants of the material. In the case of 3%Si-Fe, these constants are $\lambda_{100} = 23 \times 10^{-6}$ and $\lambda_{111} = -4.5 \times 10^{-6}$. The initial distribution of magnetic domains is strongly dependent on the magnetocrystalline energy

Manuscript received June 20, 2009; revised August 30, 2009; accepted September 02, 2009. Current version published January 20, 2010. Corresponding author: O. Hubert (e-mail: hubert@lmt.ens-cachan.fr).

Color versions of one or more of the figures in this paper are available online at http://ieeexplore.ieee.org.

Digital Object Identifier 10.1109/TMAG.2009.2032146

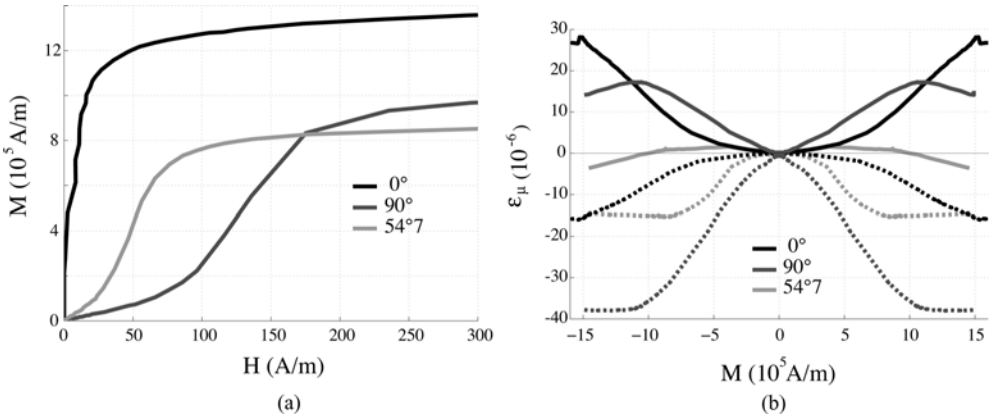

Fig. 2. Anhysteretic behavior for sample directions 0°, 90° and 54.7°—(b) full lines: $\Delta\lambda_{//}$; dashed lines: $\Delta\lambda_{\perp}$. (a) Magnetization, (b) Magnetostriction strain.

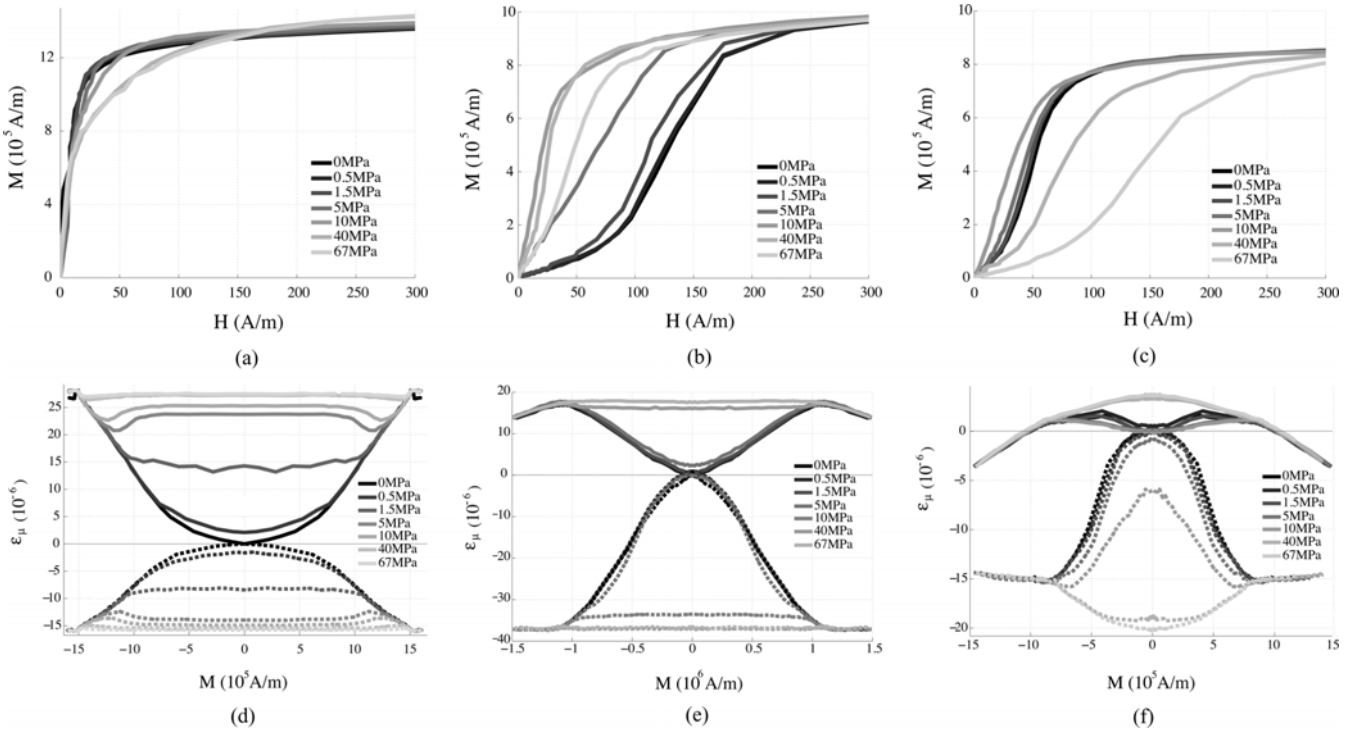

Fig. 3. Tensile stress influence on the anhysteretic behavior for sample directions 0°, 90°, and 54.7°—(d)-(e)-(f) full lines: $\Delta\lambda_{//}$; dashed lines: $\Delta\lambda_{\perp}$. (a) 0° Magnetization, (b) 90° Magnetization, (c) 54.7° Magnetization, (d) 0° Magnetostriction strain, (e) 90° Magnetostriction strain, (f) 54.7° Magnetostriction strain.

W_K^{α}, given by (3) in the case of a cubic crystal. K_1 and K_2 are the anisotropy constants of the material, respectively 35 kJ/m^3 and almost zero in the case of 3%Si-Fe

$$W_K^{\alpha} = K_1\left(\gamma_1^2\gamma_2^2 + \gamma_2^2\gamma_3^2 + \gamma_3^2\gamma_1^2\right) + K_2\left(\gamma_1^2\gamma_2^2\gamma_3^2\right). \quad (3)$$

This energetic term explains why the ideal single crystal can be divided into six domain families with magnetization respectively aligned along the six $\langle 100\rangle$ directions. But the presence of free surfaces on the sheet unbalances the ideal configuration [3] and leads to a two-domain structure along the rolling direction, schematically presented in Fig. 4(a). Starting from this initial GOSS distribution, we can write the associated magnetostriction tensor (without any loading) of the single crystal in the crystallographic frame:

$$\varepsilon_{\text{ini}}^{\mu} = \begin{pmatrix} -\frac{1}{2}\lambda_{100} & 0 & 0 \\ 0 & -\frac{1}{2}\lambda_{100} & 0 \\ 0 & 0 & \lambda_{100} \end{pmatrix}_{\text{CF}}. \quad (4)$$

If a magnetic or mechanical loading is applied, this magnetostriction tensor is changed in $\varepsilon_{\text{new}}^{\mu}$. The correspondence with experimental measurements is so that $\Delta\lambda_{//} = {}^t\vec{n}\cdot(\varepsilon_{\text{new}}^{\mu} - \varepsilon_{\text{ini}}^{\mu})\cdot\vec{n}$ and $\Delta\lambda_{\perp} = {}^t\vec{t}\cdot(\varepsilon_{\text{new}}^{\mu} - \varepsilon_{\text{ini}}^{\mu})\cdot\vec{t}$ where $\vec{n}$ and $\vec{t}$ denote the directions along sample length and width, respectively (see Fig. 4).

A. Magnetic Field Influence

The influence of the magnetic field $\vec{H}$ on the magnetic microstructure is driven by the Zeeman energy:

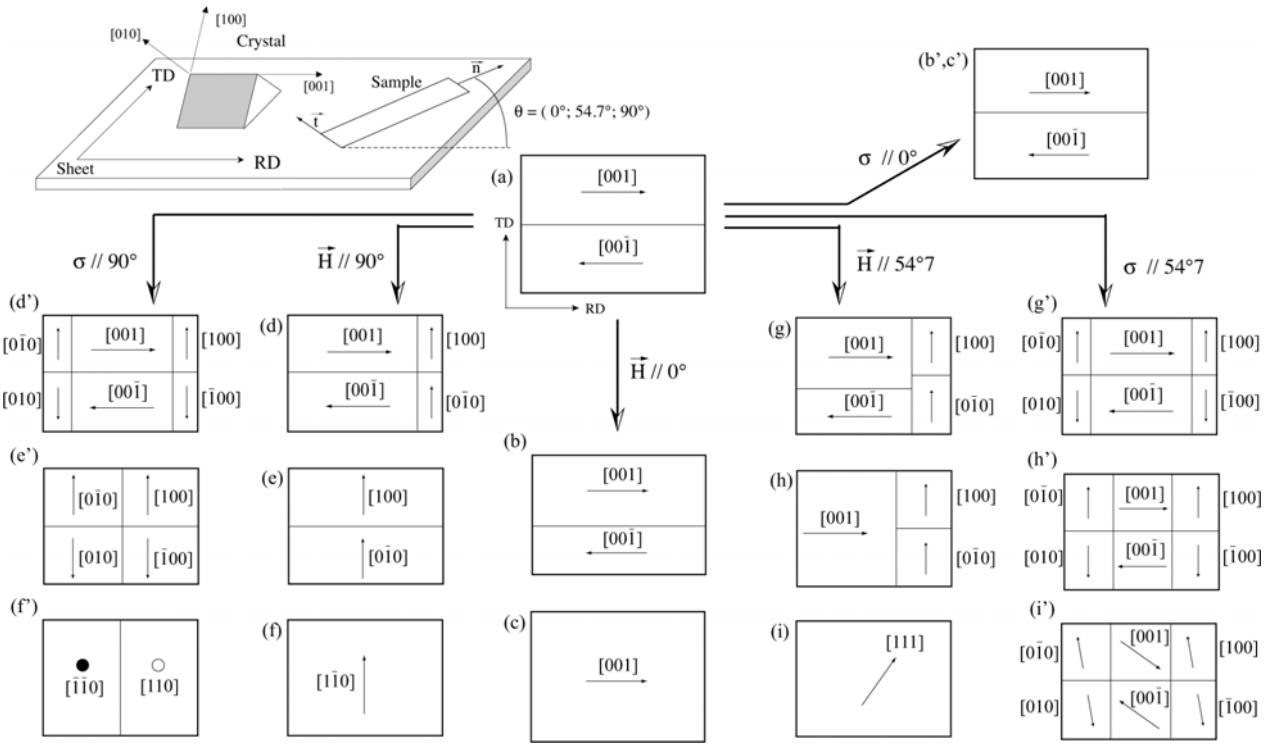

Fig. 4. Schematic representation of magnetic domain structure under magneto-mechanical loadings along three selected directions of the sheet plane (RD $=$ $0° \approx [001]$, TD $= 90° \approx [1\bar{1}0], 54.7° \approx [1\bar{1}1]$).

$$W_H^{\alpha} = -\mu_0 \vec{H} \cdot \vec{M}_{\alpha}. \tag{5}$$

The application of a magnetic field will increase the size of domains with magnetization oriented nearby the direction of the field and favor the rotation of magnetization towards this orientation.

1) $\vec{H}//0°$: domain wall motion 4(b) until magnetic saturation 4(c). Since the magnetostriction is not sensitive to the sign of the magnetization but only to its direction, this loading should not modify the magnetostriction so that $\Delta\lambda_{//} = \Delta\lambda_{\perp} = 0$. Our measurement (Fig. 3(d)) is not consistent with this scenario and rather looks like the behavior of a classical single crystal [3]. The possible explanations are the proximity of a grain boundary and/or influence of residual stresses, leading to closure domains and lancets with magnetization oriented orthogonally to the sample length in the area of the strain gage.

2) $\vec{H}//90°$: nucleation of domains in two easy magnetization directions close to the magnetic field direction 4(d); then disappearance of the initial domains 4(e); finally rotation of the two remaining domains towards the magnetic field direction 4(f). At intermediate configuration 4(e), magnetostriction tensor is given by (6), we then have: $\Delta\lambda_{//} = (3)/(4)\lambda_{100} \approx 17\times10^{-6}$ and $\Delta\lambda_{\perp} = -(3)/(2)\lambda_{100} \approx -34 \times 10^{-6}$. Experimental results are in good agreement with this scenario. The small difference can be explained by a nonideal initial configuration, for instance due to a weak crystal disorientation. At saturation 4(f), magnetostriction tensor is given by (7): we obtain $\Delta\lambda_{//} = (3)/(4)\lambda_{100}+(3)/(4)\lambda_{111} \approx 14\times10^{-6}$; theoretical value along width is unchanged: $\Delta\lambda_{\perp} = -(3)/(2)\lambda_{100} \approx -34 \times 10^{-6}$. This is consistent with the fact that we observe on Fig. 3(e) a small variation for the magnetostriction along sample length at high magnetic fields whereas the magnetostriction along sample width remains constant

$$\varepsilon_{4e}^{\mu} = \begin{pmatrix} \frac{1}{4}\lambda_{100} & 0 & 0 \\ 0 & \frac{1}{4}\lambda_{100} & 0 \\ 0 & 0 & -\frac{1}{2}\lambda_{100} \end{pmatrix}_{\mathrm{CF}} \tag{6}$$

$$\varepsilon_{4f}^{\mu} = \begin{pmatrix} \frac{1}{4}\lambda_{100} & -\frac{3}{4}\lambda_{111} & 0 \\ -\frac{3}{4}\lambda_{111} & \frac{1}{4}\lambda_{100} & 0 \\ 0 & 0 & -\frac{1}{2}\lambda_{100} \end{pmatrix}_{\mathrm{CF}}. \tag{7}$$

3) $\vec{H}//54.7°$: nucleation of domains in two easy magnetization directions close to the magnetic field direction 4(g); then coexistence of the three most favorably oriented domains 4(h); final rotation of magnetization towards the magnetic field direction at high fields 4(i). At intermediate configuration 4(h), magnetostriction tensor is given by (8): we have: $\Delta\lambda_{//} = 0$ and $\Delta\lambda_{\perp} = -(1)/(2)\lambda_{100} \approx -11 \times 10^{-6}$. At saturation 4(i), magnetostriction tensor is given by (9). Then $\Delta\lambda_{//} = \lambda_{111} \approx -4.5 \times 10^{-6}$ and $\Delta\lambda_{\perp} = -(1)/(2)\lambda_{100} - (1)/(3)\lambda_{111} \approx -10 \times 10^{-6}$. This scenario is in good agreement with the measurements of Fig. 3(f)

$$\varepsilon_{4h}^{\mu} \approx \varepsilon_{4e}^{\mu} \tag{8}$$

$$\varepsilon_{4i}^{\mu} = \begin{pmatrix} 0 & -\frac{\lambda_{111}}{2} & \frac{\lambda_{111}}{2} \\ -\frac{\lambda_{111}}{2} & 0 & -\frac{\lambda_{111}}{2} \\ \frac{\lambda_{111}}{2} & -\frac{\lambda_{111}}{2} & 0 \end{pmatrix}_{\mathrm{CF}}. \tag{9}$$

B. Tensile Stress Influence

The influence of the stress $\boldsymbol{\sigma}$ on the magnetic microstructure is driven by the magneto-elastic energy:

$$W_{\sigma}^{\alpha} = -\boldsymbol{\sigma} : \boldsymbol{\varepsilon}_{\mu}^{\alpha}. \tag{10}$$

In the case of 3%Si-Fe GO, the application of a tensile stress will increase the size of domains with magnetization oriented nearby the direction of the applied stress and can induce magnetization rotation. These two mechanisms are sequenced (volume variation at low stress, rotation at high stress) which allows a two-step analysis. The wall motion mechanism under stress is not sensitive to the sign of the magnetization but only to its direction. The mechanism of magnetization rotation under stress is much more difficult to handle than rotation under the action of a magnetic field. Let us consider a two-dimensional case and a domain initially oriented along [001] (corresponding to the case of GO sheet), and a stress σ applied along direction $\vec{n}$. The angle between $\vec{n}$ and [001] is noted ϕ_c and the angle between the magnetization and its initial position [001] is noted ϕ_1. The angle ϕ_1 can be written [5] according to

$$\phi_1(\sigma) = \frac{\operatorname{atan}(\frac{3}{2}\lambda_{111}\sigma \sin(2\phi_c))}{2K_1 + 3\lambda_{100}\sigma\cos(2\phi_c)}. \tag{11}$$

In the case of 3%Si-Fe (high K_1, $\phi_c > 0$ and $\lambda_{111} < 0$), a tensile stress will deviate the magnetization from the loading direction. The effect of stress on the magnetic behavior can finally be deduced indirectly from the observation of the evolution with stress of the projection along the magnetic field direction of the magnetization of favorably oriented domains: the stronger the projection, the higher the susceptibility. Moreover, one can remark that the effect of stress on magnetostriction leads to an initial deformation associated to the so-called ΔE effect [6].

1) $\sigma//0°$: the stress has no effect, structure is unchanged 4(b')–(c') so that $\Delta\lambda_{//} = \Delta\lambda_{\perp} = 0$. The magnetic behavior is expected to be unchanged. The experimental results [Fig. 3(d)] are not in agreement with this scenario for the same reasons detailed in Section III-A1. The application of a small tensile stress seems to realign the structure into a GOSS configuration. After the preload, we obtain $\Delta\lambda_{//} = \Delta\lambda_{\perp} = 0$ as expected. The decrease of susceptibility for stress level beyond 40 MPa is on the other hand the signature of a disorientation of the grain compared to the ideal orientation.

2) $\sigma//90°$: nucleation of orthogonal domains 4(d'); then disappearance of the initial domains 4(e'); finally rotation of magnetization away from the stress direction 4(f'). For the intermediate situation 4(e'), the magnetostriction tensor is identical to the one given by (6). It means that it is possible to mechanically saturate the magnetostriction strain to the value $\Delta\lambda_{//} = (3)/(4)\lambda_{100} \approx 17 \times 10^{-6}$ and $\Delta\lambda_{\perp} = -(3)/(2)\lambda_{100} \approx -34\times10^{-6}$. The magnetic saturation leads to the same configuration than without mechanical loading $\Delta\lambda_{//} = ((3)/(4)\lambda_{100} + (3)/(4)\lambda_{111}) \approx 14 \times 10^{-6}$. The magnetostriction along the sample width is unchanged compared to intermediate configuration 4(e'). The experimental measurements (Fig. 3(e)) confirm that it is possible to mechanically saturate magnetostriction in the absence of magnetic field. The magnetization rotation under stress is limited by free surface effect. This latter process should decrease the material susceptibility. Thus, we expect the magnetic susceptibility to increase with stress until the rotation process appears and then to decrease. This schematic view is in good agreement with the results of Fig. 3(b).

3) $\sigma//54.7°$: nucleation of orthogonal domains 4(g'); then the structure tends towards a six-domain structure similar to a single crystal structure 4(h'); finally rotation of the magnetization away from the stress direction 4(i'). For the intermediate situation 4(h'), the magnetostriction tensor is probably similar to the one obtained under a magnetic field ((8)). Consequently a magnetic loading will only introduce 180° wall motion, without deformation: the longitudinal measurement will remain zero and will undergo a rotation identical to the one observed without stress. The stress will induce an initial deformation along the sample width $\Delta\lambda_{\perp} = -(1)/(2)\lambda_{100} \approx -11 \times 10^{-6}$, corresponding to a mechanical saturation (no effect of field level except for the rotation). The rotation at high stress is more favorable for this orientation than for the 90° direction. It is difficult to express analytically the intermediate configuration. We expect saturation values identical to those obtained with no applied stress. Concerning the magnetic behavior, we expect a susceptibility increasing with stress until rotation occurs, and then a decrease, stronger than in the case of a loading along the 90° direction. The experimental measurements [Fig. 3(c)] are in good agreement with this scenario, and reveals that rotation occurs as soon as a 10 MPa stress is reached.

IV. Conclusion

In this paper, measurements of magnetization and magnetostriction strain of iron-silicon single crystals submitted to tensile stress have been presented. Results are roughly in accordance with theoretical interpretations based on domains structure evolution. The discrepancies observed denote the crucial role of the initial domains configuration and the extreme sensitivity of results to experimental procedure.

References

[1] M. J. Sablik and D. C. Jiles, *IEEE Trans. Magn.*, vol. 29, no. 3, p. 2113, May 1993.
[2] L. Daniel, O. Hubert, N. Buiron, and R. Billardon, *J. Mech. Phys. Solids*, vol. 56, p. 1018, 2008.
[3] O. Hubert and L. Daniel, *J. Magn. Magn. Mater.*, vol. 320, p. 1412, 2008.
[4] O. Hubert, L. Daniel, and R. Billardon, *J. Magn. Magn. Mater.*, vol. 254–255, p. 352, 2003.
[5] S. Lazreg and O. Hubert, in *Proc. Colloque national MECAMAT*, Aussois, 2009.
[6] L. Daniel and O. Hubert, *EPJ Appl. Phys.*, vol. 45, p. 31101, 2009.